

RECENT ADVANCES IN RADIO FREQUENCY MAGNETIZED PLASMA SPUTTERING SOURCES BASED ON EFFECTIVE TARGET UTILIZATION

^{1, 3*}MD. AMZAD HOSSAIN, ^{2,3}MD. ABDUL MAJED PATWARY, ¹MD. MUSTAFIZUR RAHMAN and ¹FATEMA TUZ ZAHURA.

¹Department of Electrical and Electronic Engineering, Jashore University of Science and Technology, Jashore -7408, Bangladesh,

²Department of Chemistry, Comilla University, Comilla -3506, Bangladesh,

³Graduate School of Science and Engineering, Saga University, Saga, 840-8502, Japan.

Abstract

In this study, the introduction of plasma and its various typical parameters were discussed. The advantages and disadvantages of radio-frequency (RF) magnetized plasma sputtering sources based on effective target utilization were presented. It was shown that the effect of the plasma sheath in RF magnetized plasma sputtering sources decreases the plasma density near the chamber wall. The principle of magnetron sputtering, demonstrating the direction of electric and magnetic fields, charged particle motions, and target erosion, was demonstrated. The direction of $\mathbf{E} \times \mathbf{B}$ drift motion in the presence of electric and magnetic fields and its role in producing plasma discharges were presented. The conventional and current research of magnetron sputtering systems was discussed. Moreover, functional thin film deposition using plasma sputtering sources and its background, as well as problems associated with effective target utilization, were discussed in detail.

Keywords: Plasma, Magnetized, Sputtering Sources, Target Utilization, Thin Film

INTRODUCTION

Plasma and Its Typical Features

A plasma is a collection of free charged particles (electrons and ions) moving in a random direction that are electrically neutral ($n_e \approx n_i$) where n_e and n_i are the electron and ion densities, respectively [1-2]. Artificially, plasma can be generated by heating or subjecting a neutral gas to a strong electromagnetic field to the point where an ionized gaseous particle becomes electrically conductive, and the behavior of the matter is dominated by the electromagnetic fields in long-range [3]. Plasma is matter heated beyond its gaseous state, heated to a temperature so high that atoms are stripped of at least one electron in their outer shells so that what remains are positive ions in a sea of free electrons. That is, as the temperature increases, the atoms become more energetic and transform matter in the sequence: solid, liquid, gas, and finally plasma, which justifies the title, "fourth state of matter".

Fluorescent lights contain plasma, and lightning is an example of plasma present at Earth's surface. Aside from those, we do not often encounter plasma in everyday life. However, outside the earth in the ionosphere, almost everything is in the plasma state. The aurora borealis, solar winds, magnetospheres of earth and Jupiter, gaseous

nebulae, galactic arms, quasars, pulsars, novae, black holes, fluorescent lamps, fires, and TVs are all examples of plasma [2]. The plasma ion engine is used for the flight of the space probe "Hayabusa". On the other hand, plasma processing is the most widely used chemical process in the microelectronic industry for thin film deposition and etching. Its application expands to surface modification, flat panel display fabrication, solar cells, plasma spray, plasma micro-discharge, and many other growing areas [4]. Recently, studies such as sterilization, surface modification, and growth stimulation of the plant have been pushed forward. It is highly advanced and the imminent products of this plasma process technology.

Figure 1 shows the schematic view of a plasma showing charged particles movements in random directions. In general, plasmas have the following characteristics [1]: (1) they are driven by a voltage or current source, electrically; (2) charged particles collisions with neutral gas molecules are significant; (3) there are boundaries at which surface losses are significant; (4) in the steady state, ionization of neutrals sustains the plasma; and (5) the electrons and the ions are not in thermal equilibrium [1-2].

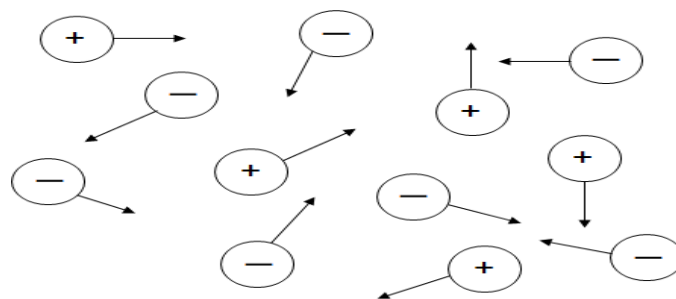


Figure 1. Schematic view of a plasma showing charged particles movements in random directions [1-2].

Figure 2 shows a typical radio-frequency (RF) plasma discharge system. It involves a voltage source that flows current through a low-pressure gas between two parallel conducting plates. The gases break down to form a typical plasma, usually weakly ionized. Plasma is formed between the electrodes. As illustrated in Fig. 2, the process chamber can be surrounded by dc multipole magnetic fields to improve plasma confinement near the chamber surfaces while maintaining a magnetic near-field-free plasma atmosphere at the wafer. Such plasma arrangements are often called remote sources [1]. Sometimes, the source and process chambers are more complex. For example, the wafer is kept very near to the source exit to obtain increased ion and radical fluxes, reduced spread in ion energy, and improved process uniformity. But the wafer is then exposed to higher levels of damaging radiation. Although the need for low pressures, high fluxes, and controllable ion energies has motivated high-density source development, there are many issues that need to be resolved [1]. A critical issue is achieving the required process uniformity over 300 mm wafer diameters. In contrast to the nearly one-dimensional geometry of typical RF diodes (two closely spaced parallel

electrodes), high-density cylindrical sources can have length-to-diameter ratios of order or exceeding unity. Plasma formation and transport in such geometries are inherently radially nonuniform [1].

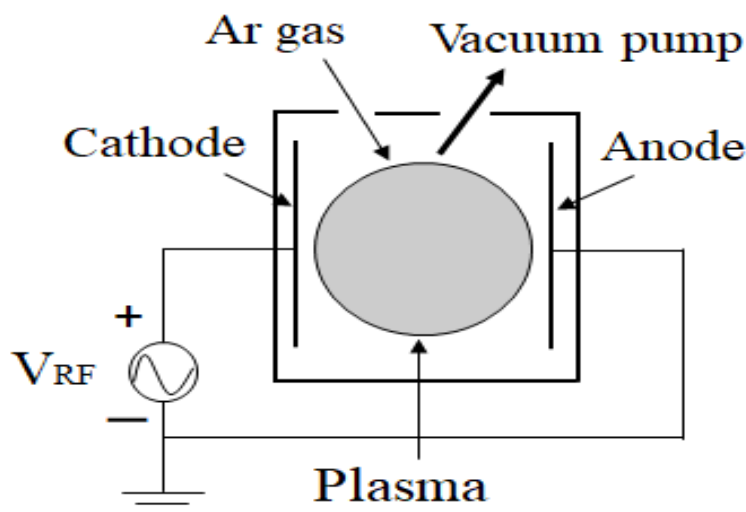


Figure 2. A typical radio-frequency plasma discharge system [1-2].

There is a wide range of densities and temperatures for both artificially processed and space plasmas. Low-pressure plasma discharges are characterized by plasma density, $n \approx 10^{14} - 10^{19} \text{ m}^{-3}$, and electron temperature, $T_e \approx 1 - 10 \text{ eV}$, which are used as chemically reactive etchants, and functional film deposition precursors. In general, while energy is delivered in the form of bombarding ions to the substrate surface, the energy flux enhances the chemistry at the substrate surface, does not heat the substrate. The functional gas pressure for these discharges is $\leq 1 \text{ Pa} - 133.3 \text{ Pa}$, and they are subjected to this study.

High-pressure discharges having $T_e \approx 0 - 2 \text{ eV}$, and $n \approx 10^{20} - 10^{25} \text{ m}^{-3}$ are also used in plasma processing. The light and heavy particles are more nearly in thermal equilibrium, satisfying the condition $T_i \leq T_e$. These discharges are used mostly to distribute heat to the substrate surface to increase surface reaction rates, to melt, evaporate materials, to weld refractory materials. The operating pressures are approximately atmospheric pressure, $1.01325 \times 10^5 \text{ Pa}$. Shock tubes, focus, high-pressure arcs, and laser plasma are examples of high-pressure discharges that have a plasma density of approximately $n \approx 10^{20} \text{ m}^{-3}$. Fusion reactor plasmas ($n \approx 10^{20} - 10^{21} \text{ m}^{-3}$, and $T_e \approx 3.5 - 4 \text{ eV}$), alkali metal plasmas ($n \approx 10^{15} - 10^{18} \text{ m}^{-3}$, and $T_e \approx 1 \text{ eV}$), flames ($n \approx 10^{14} \text{ m}^{-3}$, and $T_e \approx 1 \text{ eV}$), earth ionosphere ($n \approx 10^{10} - 10^{14} \text{ m}^{-3}$, and $T_e \approx 2 \text{ eV}$) and laser plasma ($n \approx 10^{25} - 10^{27} \text{ m}^{-3}$, and $T_e \approx 2 - 3 \text{ eV}$), are typical examples of various plasma discharges [1-2].

Plasma Sheaths and Debye Length

Figure 3 shows the profile of the densities after the formation of the sheath near the chamber wall. The condition $n_e \approx n_i$ is called quasi-neutrality and is one of the most important characteristics of plasma [1-2]. Plasmas are quasi-neutral ($n_e \approx n_i$), and are joined to chamber wall surfaces across thin positively charged layers called sheaths.

The plasma potential varies slowly in the plasma but rapidly in the sheath. The plasma density is relatively flat in the center and falls sharply near the sheath edge. The electron densities fall rapidly at the chamber wall surface. If the sheath potential drops are unequal, the electron fluxes will also be unequal. The Bohm criterion states that ions must stream in the plasma sheath with a minimum velocity of $(kT_e/M)^{1/2}$ [2].

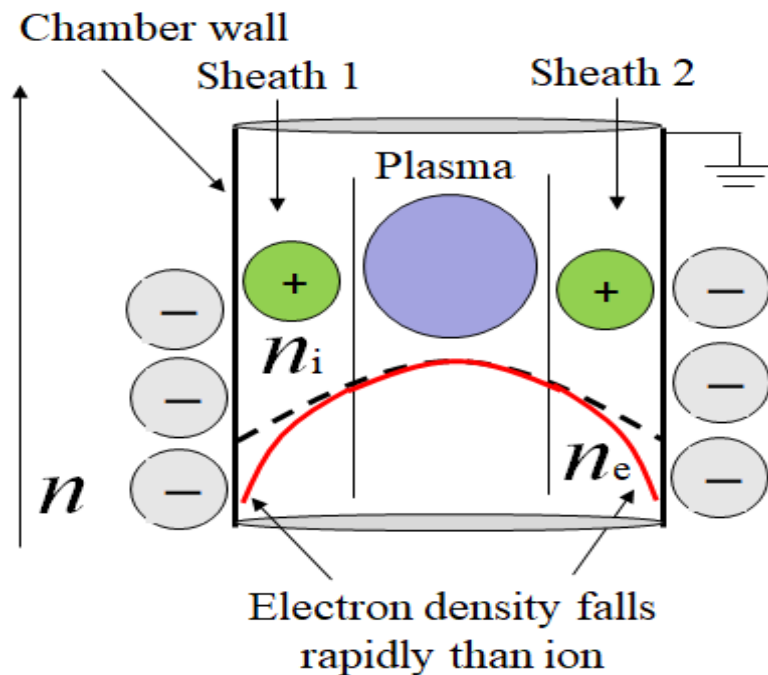


Figure 3. Profile of the densities after formation of the sheath near the chamber wall [1-2]

A fundamental characteristic of the behavior of a plasma is its ability to shield out the electric potentials of individual charged particles that are applied to it. Debye length indicates the distance scale over which significant charge densities can spontaneously exist. The characteristic length scale in a plasma is the Debye length, λ_D can be represented by the following equation [1-2].

$$\lambda_D = \left(\frac{\epsilon_0 T_e}{q n_0} \right)^{1/2} \quad (1)$$

Debye length increases, when electron temperature, T_e rises. It is assumed that plasma having equilibrium densities $n_e = n_i = n_0$. In practical units, it can be written as following form [1]:

$$\lambda_D \approx 743\sqrt{T_e/n_e} \quad (2)$$

With T_e in electron volts and n_e in cm^{-3} . For example, Debye length is 0.14 mm for $T_e = 4$ eV and $n_e = 10^{10} \text{cm}^{-3}$.

Cyclotron Frequency and Larmor Radius

If the plasma is inserted into a DC magnetic field (\mathbf{B} -field), the motions of the charged particles are affected by the \mathbf{B} -field which makes the plasma an anisotropic medium, with a preferred direction along \mathbf{B} -field. That is, the charged particle, electron rotates along the \mathbf{B} -field as shown in figure 5. As long as the ion or electron of charge q is moving, it experiences a Lorentz force, $q\mathbf{v} \times \mathbf{B}$, which is perpendicular to both velocity and the field. This force has no effect on the velocity component of \mathbf{B} -field, but in the perpendicular plane, it powers the particle to rotate in a cyclotron orbit. The frequency of this circular motion, the cyclotron frequency, ω_c is represented by the following equation [2].

$$\omega_c = qB/m \quad (3)$$

The radius of the circle of rotation called the Larmor radius or gyro-radius, r_L . The cyclotron frequency is independent of velocity. However, gyro-radius, r_L depend on velocity. If v is the velocity component in the plane perpendicular to \mathbf{B} -field, a particle completed an orbit a length, $2\pi r_L$ in a time, $2\pi/\omega_c$, so $v = r_L \omega_c$, alternatively, it can be written by the following formulae [1-4].

$$r_L = v/\omega_c \quad (4)$$

$$r_L = mv/qB \quad (5)$$

That is, the presence of the \mathbf{B} -field controls the charged particles, in especial, electrons, so that electrons are magnetized. The magnetized electrons play an important role in producing a high-density plasma that can enhance the deposition rate for plasma processing such as plasma sputtering. Figure 4 shows the rotation of an electron in the presence of a magnetic field. The Larmor radius can be controlled by the velocity, v and the magnetic field, B , respectively.

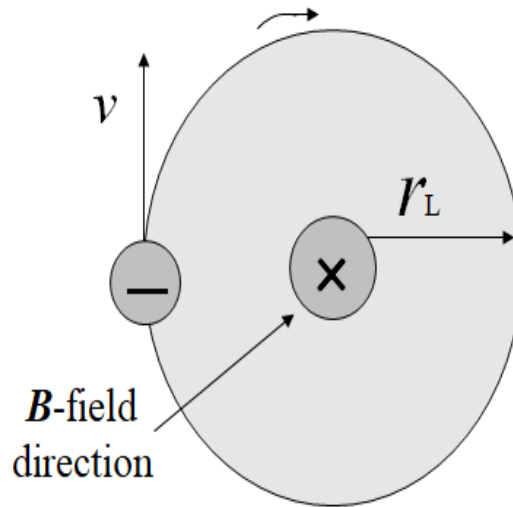


Figure 4. Rotation of electron in the presence of the magnetic field [1-2].

$E \times B$ Drift Motion

The direction of the electric field, E and the behavior of magnetic flux density, B play an important role in performing the magnetized discharge based on $E \times B$ drift motion, where E and B are the electric field perpendicular to the target and magnetic flux density parallel to the target, respectively. The direction of $E \times B$ drift motion in the presence of electric and magnetic field is shown in figure 5. Moreover, it can be demonstrated by the right hand rule. If the magnetic fields are so strong that both ions and electrons have Larmor radii much smaller than the plasma radius. So that the particles guiding centers drift across the B -field, in response to applied electric fields, E , the perpendicular component to B -field. The drift velocity can be found using the following Eq. (6). The velocity component parallel to the B -field is unaffected by the E -field. Moreover, the drift velocity, v , is perpendicular to both the E -field and the B -field and has the same value for ions and electrons.

$$v = \frac{E \times B}{|B|^2} \quad (6)$$

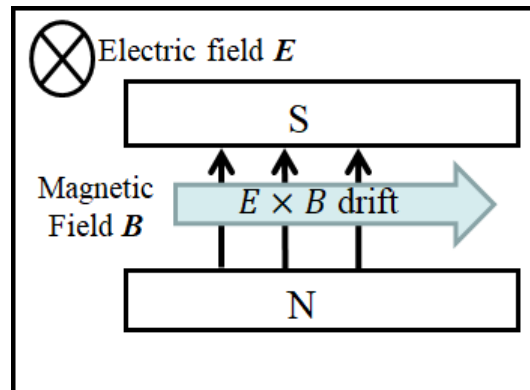


Figure 5. Direction of $E \times B$ drift motion in the presence of electric and magnetic field [1].

Thin Film Deposition by Plasma Sputtering

Principle of Plasma Sputtering

Sputter deposition is a physical vapor deposition (PVD) method of thin film deposition. This process consists of ejecting material from a target surface onto a substrate. Sputtered atoms ejected from the target surface have a wide energy distribution, typically up to tens of eV (100,000 K). The number of atoms ejected or “sputtered off” from the target surface is called the sputter yield. The sputter yield depends on the energy and incident angle of the bombarding ions, the relative masses of the ions and target atoms, and the surface binding energy of the target atoms. Plasma processing such as plasma CVD and sputtering is widely used for the fabrication of microelectronic thin films preparation. Magnetron sputtering has become the process of choice for the deposition of a wide range of industrially important coatings. Figure 6 shows the principle of magnetron sputtering, demonstrating the direction of electric, and magnetic fields, charged particle motions, and target erosion. Magnetron sputtering is a plasma vapor deposition (PVD) process in which a plasma is created and positively charged ions from the plasma are accelerated by an electrical field superimposed on the negatively charged electrode or “target”. The positive ions are accelerated by potentials ranging from a few hundred to a few thousand electron volts and strike the negative electrode with sufficient force to dislodge and eject atoms from the target. These atoms will be ejected in a typical line-of-sight cosine distribution from the face of the target and will condense on surfaces that are placed in proximity to the magnetron sputtering cathode. A magnetic field is applied at right angles to the electric field by placing large magnets behind the target. This traps electrons near the target surface and causes them to move in a spiral motion until they collide with an Ar atom. To increase deposition rates, magnets are used to increase the percentage of electrons that take part in ionization events, increasing the ionization efficiency. The orbital motion of electrons increases the probability that they will collide with neutral species and create ions [3-4].

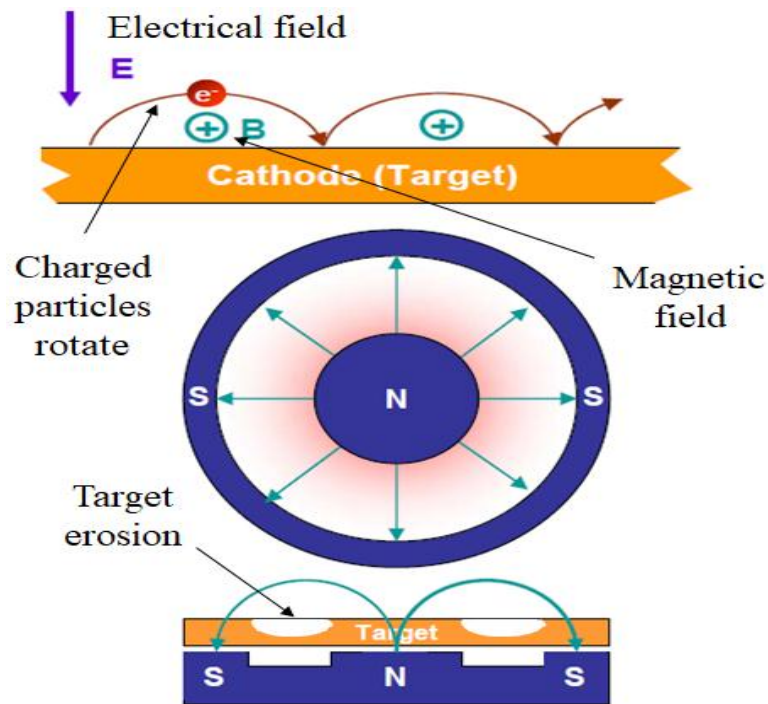


Figure 6. Principle of magnetron sputtering demonstrating the direction of electric, magnetic field, charged particle motions and target erosion [4].

Merits and Demerits of Plasma Sputtering

Magnetron sputtering sources are very familiar plasma sources for functional thin film preparation such as metal, oxide, nitride, and nano-material thin films. The merits of magnetron sputtering sources are high-speed deposition rate and high-quality thin film properties. However, the major demerits are non-uniform target erosion profile and lower target utilization rate, such as 30-40% due to localized ring-shaped high-density plasma. So, it is needed to develop a novel plasma sputtering source with an improved target utilization percentage, erosion rate, and uniform film property. Many researchers are doing research to improve target utilization percentage [4].

Background Research on Radio Frequency Plasma Sputtering

Synthesis of Functional Films by Plasma Sputtering

Cu films of 290–350 nm were prepared by DC magnetron sputtering, at a target voltage of 400 V, and Ar gas pressure was introduced at 0.5, 1.0, and 1.5 Pa, respectively, by H. Qiu et al. [5]. It was found that the target current increased from 69 to 200 mA with increasing Ar pressure, and the target voltage was settled at 400 V. The amount of larger grains decreases with an increase in Ar pressure while the resistivity of the films increases with increasing Ar pressure. The roughness of the film surface was approximately 5 nm, which was independent of Ar pressure [5]. The crystalline

orientation of the prepared Cu film shifted slightly from the [1 1 1] direction to the [2 2 0] direction with increasing Ar pressure [5].

Cu doped ZnO films at various doping concentrations of Cu (0, 5.1, 6.2 and 7.5%) by simultaneous RF and DC magnetron were prepared by A. Sreedhar et al. [6]. The structural, electrical, and optical properties of ZnO films were discussed in detail. X-ray diffraction (XRD) patterns show that the films were polycrystalline in nature with a wurtzite structure toward the c-axis, and atomic force microscopy (AFM) results indicate that the films displayed needle-like shaped grains throughout the substrate surface. The electrical resistivities were found to be increased with an increase of copper content from 0 to 7.5% [6]. Films showed an average optical transmittance of about 80% in the visible region and optical band gap values decreased from 3.2 to 3.01 eV with an increasing of Cu doping content from 0 to 7.5%, respectively [6]. However, the optical band gap values decreased from 3.2 to 3.01 eV with increasing the copper doping concentration from 0 to 7.5% in the ZnO host lattice [6].

The size effect on the resistivity of evaporated copper films, ranging in thickness from 9 nm to 167 nm, was determined experimentally from the sheet resistance and the physical thickness [7]. In combination, to determine the mean grain size of the grains in the plane of the film, the Electron Back Scatter Diffraction (EBSD) and the XRD methods were used, A. E. Yarimbiyik et al. proposed that Matthiessen's rule can be used to measure the thickness of a copper film and [7]. The resistivity of these films increased with decreasing film thickness [7].

Al-doped ZnO (AZO) thin films have been prepared by radio frequency (RF) magnetron sputtering and applied RF power was varied in the range of 600–1200 W by A. Spadoni et al. [8]. The effects of RF power on structural, electrical, and optical properties were examined by XRD analysis, Hall measurements, and UV–vis–NIR spectrophotometry, respectively. It was found that increasing the RF power, AZO films having a preferential growth orientation along (002) direction, showed a decrease of the lattice distance indicating a less defected structure [8]. It was observed that the increase in the RF power made a higher optical absorption by free carriers, coupled with an increase in the band gap value. Resistivity varied from $1.1 \times 10^{-3} \Omega \text{ cm}$ at 600 W down to a minimum value of $5.6 \times 10^{-4} \Omega \text{ cm}$ at 1200 W, whereas the carrier density increased up to $1 \times 10^{21} \text{ cm}^{-3}$. The lattice defect variation of AZO films was analyzed by photoluminescence (PL) measurements. It was hypothesized that at higher RF power a more effective diffusion phenomenon can give more effective Al doping and less amount of zinc vacancies. As a consequence, Al atoms are more effectively trapped into the structure [8].

S. Rahmane et al. deposited Al-doped ZnO (AZO) films on glass and silicon substrates by an RF magnetron sputtering technique at room temperature [9]. The effects of thickness on the structural, optical and electrical properties were investigated. It was found that the electrical resistivity decreases with the increase of the film thickness and the smallest measured value was $8 \times 10^{-4} \Omega \text{ cm}$ for the 1500 nm thick film. All the deposited films showed a crystalline wurtzite structure with a strong preferred (002) orientation. It was observed that the intrinsic compressive stress decreased with the

increase of the film thickness [9]. The obtained AZO films had an average transmittance greater than 90% in the visible region, and films have an optical band gap between 3.32 and 3.49 eV depending on the film thickness [9].

Cu film has been proposed because of its low resistivity, high chemical stability, and excellent electromigration resistance by B. H. Wu et al. [10]. The films deposited on a silicon substrate by varying the substrate bias voltage using high power pulsed magnetron sputtering (HPPMS). It was found that the substrate bias increased from -17.3 V to -100 V, the electron current decreased slowly, while the ion current increased, and steadied at -50 V [10]. It was observed that the Cu films prepared at -50 V, and -100 V exhibited a higher tensile stress and a superior (111) texture. The electrical resistivity of the deposited Cu films was found to be a minimum value of 1.79 $\mu\Omega\text{cm}$ at -100 V [10].

A. S. Christiansen et al. investigated the nitrogen dissociation and plasma parameters during radio frequency sputtering of lithium phosphorus oxynitride thin films in nitrogen gas by mass appearance spectrometry, electrostatic probes, and optical emission spectroscopy [11]. Despite lower plasma density, the film grows quicker at a lower pressure where the higher plasma potential, translated into higher energy for imposing ions on the substrate which resulted in a compact and smooth film structure. It was found that low pressure (5 mTorr) and moderate power (100 W) were most beneficial for the growth of good quality films with a high ionic conductivity [11]. Increasing the RF power (300W) resulted in a poor film quality due to cracks and dislocation of large clusters from the target material, while increasing the nitrogen pressure (50 mTorr) resulted in a lower deposition rate and a rough microstructure with volcano-shaped structures on the surface. Higher pressures showed much less nitrogen dissociation and lower ion energy with thinner films, less ionic conductivity, and poor film structure with large roughness [11].

A highly transparent field emitter was achieved by Ar^+ ion irradiation onto highly transparent and conducting ZnO films deposited on glass substrates by Zurita Zulkiflil et al. [12]. The deposited flat ZnO films before ion irradiation, which showed 90% transmittance and 186 Ω/cm sheet resistance, showed no field emission current up to 15 μVm^{-1} [12]. The nanocone size was less than the wavelength of visible light, and the transmittance was maintained at 86% for the ion-irradiated ZnO film [12]. It was observed that the field emission properties of the transparent nanoconed ZnO were promising and comparable to those of other nontransparent nanostructured ZnO [12].

An inverted gapped-target magnetron sputtering device for the deposition of ferromagnetic thin films under energetic conditions has been developed by P. Poolcharuansin et al. [13]. The side view and the front view pictures during the inverted plasma discharge with a power of 80 W, and a pressure of 2 Pa were discussed [13]. No cracking of the film surfaces was found in the sputtering of nickel films without substrate heating or biasing. Langmuir probe and ion energy measurements confirmed that plasma ions with a density of around 10^{16} m^{-3} and the almost energies of approximately 200 eV can be reached at the substrate [13].

A wider eroded and higher target utilized magnetron sputtering system for ferromagnetic nickel (Ni) target using a large, tall and eccentrically rotating tilted center magnet was proposed by T. Iseki et al. [14]. The target utilization was found to be approximately 49% for 5-inch and 4-mm thick Ni target, which is 8% better than when a non-tilted center magnets were used. It was observed that the rotating mechanism of a yoke magnet could be separated from the cooling water and the target could be cooled more effectively, and the center non-eroded area was decreased [14].

T. Iseki et al. investigated the dependence of the magnetic flux density, erosion uniformity, and target utilization on the yoke magnet tilt angle in a planar magnetron sputtering system, using a rotating, tilted, unbalanced, asymmetrical magnet [15]. The magnetic flux density distributions were measured two-dimensionally on the target surface. As the yoke magnet tilt angle increased from 0 to 8 degree, utilization of a 5-inch target linearly increased from 60 to 80%. On the other hand, with an elliptical outer yoke, the target utilization was approximately 70%, regardless of the yoke magnet tilt angle [15]. It was found that the deposition rate when using the elliptical outer yoke was 1.2 times faster than that of when using the circular outer yoke at the same magnet tilt angle [15]. However, to make a tilt angle on a yoke surface, an unbalanced magnet is arranged on the magnet holder surface. The number of magnets is different from one side to another side. These effect make its short system life.

Yasunori Ohtsu et al. proposed the racetrack-shaped RF magnetron plasma with weak rubber magnets (ferrite and neodymium) for the full utilization of the circular target and the reduction of the magnet weight [16]. The magnetic field simulations for the ferrite rubber magnets, the neodymium rubber magnets, and the neodymium rubber magnets including the neodymium metal magnets were investigated [16]. The radial profile of the erosion depth was roughly constant for $r = 20$ mm and then decreased slowly away from the center for an RF power of 40 W, an Ar gas pressure of 2 Pa and a sputtering time of 4 h. It was found that the target utilization was approximately 72% estimated from the target erosion profile [16].

Moreover, various plasma sputtering sources have been investigated for functional film deposition and material processing [17-28]. M. A. Hossain et al. reported that the copper target utilization percentage was achieved by 74.15% and increased to 87.49% using an iron cover to shield the magnetic fluxes [23]. It was investigated that the optical and electrical characteristics of the deposited AZO films using RF magnetized sputtering plasma source [28]. M. A. Hossain et al. investigated a RF magnetized ring-shaped plasma source using a monopole magnet arrangement [25-26]. However, the ring-shaped plasma discharges were observed in the outer circle of the chamber.

Yasunori Ohtsu et al. proposed a rotational windmill-shaped radio frequency magnetron plasma source has been developed to improve the target utilization rate. The target utilization rate has been achieved at 65% and 70% for an initial and improved magnet arrangements, respectively [29]. Y. Ohtsu et al. investigate a radio frequency double-ring-shaped hollow cathode plasma source with permanent magnets for high-density hydrogen plasma generation [30]. The discharge breakdown voltage with a magnet is

lower than that without a magnet under low gas pressure. Various plasma sources were used for functional material fabrication and industrial application [31-41].

Yasunori Ohtsu et al. prepared a water-repellent film on a plastic plate by unbalanced radio-frequency magnetron plasma sputtering using a polytetrafluoroethylene target for a next generation automobile window [42]. They found that the water contact angle is independent of RF power. Takashi Sumiyama et al. measured a spatial structure of high-density radio frequency ring-shaped magnetized discharge plasma sputtering with two facing Al-doped ZnO (AZO) cylindrical targets mounted on a ring-shaped hollow cathode [28]. AZO thin film was deposited without substrate heating for effective target utilization.

Md. Abdul Majed Patwary developed Cu oxide thin films by radio frequency magnetron sputtering in an ambient of argon and oxygen using a pure Cu target. The structural, electrical, and optical properties were investigated systematically as a function of O₂ flow rate and substrate positions by et al. [43]. It was also investigated influence of oxygen flow rate and substrate positions on properties Cu oxide thin films. After deposition on a substrate, it was then cut into several pieces based on substrate position to characterize the grown film for further examination of the pure Cu target.

Problems of the Plasma Sputtering and Objectives of this Study

Magnetron Sputtering Sources are very familiar plasma sources for functional thin film preparation such as metal, oxide, nitride and nanomaterials thin films. Recently, RF magnetized plasma sources have been widely used in microelectronics, such as magnetic films, surface treatment and cleaning, diamond-like carbon, biomaterial thin films, flat panel display fabrication, transparent conductive oxide film preparation for solar cells and mobile phones, and many other rapidly growing areas. In particular, RF magnetron plasma sources have become an attractive tool for functional film preparation. In the conventional magnetron system, the target material is not effectively used because high-density plasma is localized on the target surface. The target utilization is very low approximately at 20-30% [5].

From the practical viewpoint of the limited resources, the utilization of the target material is necessary. The symmetrical magnets magnetron sputtering method with one inner magnet and two outer annular magnets facing each other were investigated. The maximum target erosion rate was 57% [17]. The rotating magnet sputtering has also been proposed for rotating helical magnets to increase the target utilization efficiency. Using a rotating unbalanced and asymmetrical magnet, a flat erosion-sputtering method has been developed. The estimated target utilization had a value of 80% and 77% for five, four-inch aluminum target materials, respectively [13-14]. The target utilization efficiency was increased from 73.6% to 86.3% when iron pole pieces were used in the rotating cruciform arrangement of neodymium magnets [17-18].

In general, near the chamber wall, the plasma potential and the plasma density are very small because an ion sheath exists near the wall [1, 19]. The plasma potential varies slowly in the plasma but rapidly in the sheath region. Only in the sheath region can the quasineutrality property not be satisfied. The plasma density profile is relatively flat in

the center and falls sharply near the sheath edge. It is required to produce (1) outer ring-shaped and (2) specific area plasmas for obtaining (1) uniform, (2) high-density plasma as well as (3) convenient outer target area erosion profile near the chamber wall. Moreover, plasma processing has various problems with plasma equipment, thin film preparation, and so on. In practical industrial applications, the outer width of the target is large.

Therefore, it is required to have high-density plasma discharge in a specific area and also in the outer region of the chamber to obtain a convenient outer target area erosion profile near the chamber wall. Moreover, to deposit a functional thin film in a specific area near the chamber wall, the target utilization in a specific area is required from the viewpoint of target utilization. However, the conventional magnetron plasma has an issue where the target erosion is not uniform owing to high-density localized plasmas.

CONCLUSION

In this study, the developments of various novel plasma source equipment with uniform target utilization were discussed for the growing plasma processing applications. Various important plasma parameters were discussed in detail. The effects of plasma sheath, larmor radius, and cyclotron frequency were presented. The following aims and objectives of this study were given priority, such as (a) study of finding a way of increasing target utilization percentage, (b) study of making a uniform target erosion over the entire area of the target, (c) study of depositing a uniform functional film property, and (d) study of producing a specific area plasma for target utilization near the chamber wall. Various functional thin film preparation and their characterization processes were demonstrated. Recent advances in RF magnetized plasma sputtering sources based on effective target utilization for functional film deposition and industrial applications were discussed in detail.

ACKNOWLEDGMENT

The authors would like to thank Professor Dr. Yasunori Ohtsu, Graduate School of Science and Engineering, Saga University, Japan for supervisions and guidelines and also Professor Dr. Hirota Toyoda, Nagoya University, Japan, for fruitful discussions. Moreover, Dr. Hossain extends his gratitude to Mr. Tsubasa Ide, Mr. Yutaro Nakamura and Mr. Kosei Sugawara, Graduate School of Science and Engineering, Saga University, Saga, 840-8502, Japan for their comments and suggestions.

Ethical Responsibility of Authors: The authors declare the Ethical Responsibility of Authors.

Conflicts of Interests: The authors declare there are no conflicts of interests and no competing interests.

REFERENCES

1. M. A. Lieberman, and A. J. Lichtenberg, "Principles of Plasma Discharges and Material Processing", 2nd ed. John Wiley & Sons, Inc., New York, 2005.
2. F. F. Chen, and J. P. Chang, "Lecture Notes on Principles of Plasma Processing", Plenum, New York, 2002.

3. A. I. Morozov, "Introduction to Plasma Dynamics", CRC Press, 2012.
4. Hossain Md. Amzad, "Development of Magnetized Plasma Sputtering Source for Effective Target Utilization with Various Magnet Setups", PhD Thesis, Graduate School of Science and Engineering, Saga University, Japan, September 2018.
5. H. Qiu, F. Wanga, P. Wua, L. Pana, and Y. Tiana, Vacuum, 66, 447–452, 2002.
6. A. Sreedhar, J. H. Kwon, J. Yi, J. S. Kim, and J. S. Gwag, Materials Science in Semiconductor Processing, 49, 8–14, 2016.
7. A. E. Yarimbiyik, H. A. Schafft, R. A. Allen, M. D. Vaudin, and M. E. Zaghloul, Microelectronics Reliability, 49, 127–134, 2009.
8. A. Spadoni, and M.L. Addonizio, Thin Solid Films, 589, 514–520, 2015.
9. S. Rahmane, M. S. Aida, M. A. Djouadi, and N. Barreau, Superlattices and Microstructures, 79, 148–155, 2015.
10. B. H. Wu, J. Wu, F. Jiang, D. L. Ma, C. Z. Chen, H. Sun, Y. X. Leng, and N. Huang, Vacuum, 135, 93 – 100, 2017.
11. A. S. Christiansen, E. Stamate, K. Thyden, R. Younesi, and Peter Holtappels, Journal of Power Sources, 273, 863 – 872, 2015.
12. Z. Zulkifli1, S. Munisamy, M. Z. M. Yusop, G. Kalita, and M. Tanemura, Japanese Journal of Applied Physics, 52, 11NJ07, 2013.
13. P. Poolcharuansin, P. Laokul, N. Pasaja, A. Chingsungnoen, M. Horprathum, P. Chindaudom, and J. W. Bradley, Vacuum, 141, 41-48, 2017.
14. T. Iseki, H. Maeda, T. Itoh, Vacuum, 82, 1162–1167, 2008.
15. T. Iseki, Vacuum, vol. 84, pp. 339–347, 2010.
16. Y. Ohtsu, S. Tsuruta, T. Tabaru, and M. Akiyama, Surface Coatings Technology, 307, 1134–1138, 2016.
17. Y. Ohtsu, M. Shigyo, M. Akiyama, T. Tabaru, Vacuum, 101, 403 – 407, 2014.
18. Tsubasa Ide, M. A. Hossain, Y. Nakamura, and Y. Ohtsu, Journal of Vacuum Sci. Technol. A: Vacuum, Surfaces, and Films, 35, 061312, 2017.
19. P. J. Kelly, R. D. Arnell, Vacuum, 56, 159 – 172, 2000.
20. Y. Ohtsu and T. Yanagise, Plasma Sources Sci. Technol., 24, 034005, 2015.
21. Long Wen, Bibhuti B. Sahu, Hye R. Kim, Jeon G. Han, Applied Surface Science, 473 (2019) 649–656.
22. Y. Ohtsu, N. Matsumoto, J. Schulze, and E. Schuengel, Phys. Plasmas 23, 033510, 2016.
23. M. A. Hossain, T. Ide, K. Ikari, and Y. Ohtsu, Vacuum, 128, pp. 219-225, 2016.
24. M. A. Hossain, Y. Ohtsu, and T. Tabaru, Plasma Chem. Plasma Process., vol. 37, pp. 1663–1677, 2017.
25. Md. Amzad. Hossain and Yasunori Ohtsu, Jpn. J. Appl. Phys., vol. 57, 01AA05, 2018.
26. Md. Amzad. Hossain and Yasunori Ohtsu, IEEE Transaction on Plasma Sci., vol. 46, no. 8, August 2018.
27. M. A. M. Patwary, M. Ohishi, K. Saito, Q. Guo, K. M. Yu, T. Tanaka, "Effect of Nitrogen Doping on Structural, Electrical, and Optical Properties of CuO Thin Films Synthesized by Radio Frequency

- Magnetron Sputtering for Photovoltaic Application”, ECS J. Sol. State Science and Technology, 10 (2021) 065019.
28. Takashi Sumiyama, Takaya Fukumoto, Yasunori Ohtsu, and Tatsuo Tabaru, AIP Advances 7, 055310, 2017.
 29. Yasunori Ohtsu, Takahiro Nakashima, Rei Tanaka, Julian Schulze, Vacuum, vol. 181, 109593, Nov. 2020.
 30. Yasunori Ohtsu, Shoma Imoto, Shunya Takemura, Julian Schulze, Vacuum, vol. 193, 110531, Nov. 2021.
 31. H.-M. Xiong, Z.-D. Wang, D.-P. Xie, L. Cheng, Y.-Y. Xia, J. Mater. Chem. 16, 1345-1349, 2006.
 32. H. Huang, G. Fang, S. Li, H. Long, X. Mo, H. Wang, Y. Li, Q. Jiang, D.L. Carroll, J. Wang, Appl. Phys. Lett. 99, 263502, 2011.
 33. B.-Y. Oh, J.-H. Kim, J.-W. Han, D.-S. Seo, H.S. Jang, H.-J. Choi, S.-H. Baek, J.H. Kim, G.-S. Heo, T.-W. Kim, Curr. Appl. Phys.12, 273-279, 2012.
 34. J. Kim, J.-H. Yun, C.H. Kim, Y.C. Park, J.Y. Woo, J. Park, J.-H. Lee, J. Yi, C.-S. Han, Nanotechnology 21, 115~205, 2010.
 35. A. Waag, T. Gruber, K. Thonke, R. Sauer, R. Kling, C. Kirchner, H. Rössler, J. alloys Compd. 371, 77-81, 2004.
 36. D. Bhatia, H. Sharma, S. Nawaz, R. Meena, C. Tomy, V. Palkar, 2015 arXiv preprint arXiv:1506.06156.
 37. P. Sharma, S. Kumar, K. Sreenivas, J. Mater. Res. 18, 545~548, 2003.
 38. M. Dutta, D. Basak, Nanotechnology 20, 475602, 2009.
 39. K.H. Yoon, J.-W. Choi, D.-H. Lee, Thin Solid Films 302, 116~121, 1997.
 40. D.-L. Hou, R.-B. Zhao, Y.-Y. Wei, C.-M. Zhen, C.-F. Pan, G.-D. Tang, Curr. Appl. Phys. 10, 124~128, 2010.
 41. F.A. Mahmoud, G. Kiriakidis, J. Ovonic Res. 5, 15~20, 2009.
 42. Yasunori Ohtsu, Yuta Ino, Yuki Fukio, Tatsuo Tabaru, Takeshi Yasunaga, and Yasuyuki Ikegami, Plasma Chemistry and Plasma Processing, 41, 1631-1646, 2021.
 43. Md. Abdul Majed Patwary, Katsuhiko Saito, Qixin Guo, Tooru Tanaka, Thin Solid Films, 675 (2019) 59-65.